Author(s): Eronen, T.; Ge, Z.; de Roubin, A.; Ramalho, M.; Kostensalo, J.; Kotila, J.; Beliushkina, O.; Delafosse, C.; Geldhof, S.; Gins, W.; Hukkanen, M.; Jokinen, A.; Kankainen, A.; Moore, I.D.; Nesterenko, D.A.; Stryjczyk, M.; Suhonen, J.

Title: High-precision measurement of a low Q value for allowed β−-decay of 131I related to neutrino mass determination

Year: 2022

Version: Published version

Physics Letters B 830 (2022) 137135

Contents lists available at ScienceDirect

Physics Letters B

www.elsevier.com/locate/physletb

High-precision measurement of a low Q value for allowed β^--decay of ^{131}I related to neutrino mass determination

T. Eronen [a,*], Z. Ge [a,*], A. de Roubin [b], M. Ramalho [a], J. Kostensalo [c], J. Kotila [a,d,e], O. Beliushkina [a], C. Delafosse [a], S. Geldhof [a,1], W. Gins [a], M. Hukkanen [a,b], A. Jokinen [a], A. Kankainen [a], I.D. Moore [a], D.A. Nesterenko [a], M. Stryjczyk [a], J. Suhonen [a,*]

[a] Department of Physics, University of Jyväskylä, P.O. Box 35, FI-40014, Jyväskylä, Finland
[b] Centre d'Etudes Nucléaires de Bordeaux Gradignan, UMR 5797 CNRS/IN2P3 - Université de Bordeaux, 19 Chemin du Solarium, CS 10120, F-33175, Gradignan Cedex, France
[c] Natural Resources Institute Finland, Yliopistokatu 6, FI-80130, Joensuu, Finland
[d] Finnish Institute for Educational Research, University of Jyväskylä, P.O. Box 35, FI-40014, Jyväskylä, Finland
[e] Center for Theoretical Physics, Sloane Physics Laboratory, Yale University, New Haven, CT 06520-8120, USA

A R T I C L E   I N F O

Article history:
Received 5 January 2022
Received in revised form 22 April 2022
Accepted 22 April 2022
Available online 27 April 2022
Editor: D.F. Geesaman

Keywords:
Penning trap
Low Q value
β^- decay
Neutrino mass

A B S T R A C T

The ground-state-to-ground-state β^--decay ^{131}I $(7/2^+) \rightarrow$ ^{131}Xe $(3/2^+)$ Q value was determined with high precision utilizing the double Penning trap mass spectrometer JYFLTRAP at the IGISOL facility. The Q value of this β^--decay was found to be $Q = 972.25(19)$ keV through a cyclotron frequency ratio measurement with a relative precision of 1.6×10^{-9}. This was realized using the phase-imaging ion-cyclotron-resonance technique. The new Q value is more than 3 times more precise and 2.3σ higher (1.45 keV) than the value extracted from the Atomic Mass Evaluation 2020. Our measurement confirms that the β^--decay to the $9/2^+$ excited state at 971.22(13) keV in ^{131}Xe is energetically allowed with a Q value of 1.03(23) keV while the decay to the $7/2^+$ state at 973.11(14) keV was found to be energetically forbidden. Nuclear shell-model calculations with established two-body interactions, alongside an accurate phase-space factor and a statistical analysis of the $\log ft$ values of known allowed β decays, were used to estimate the partial half-life for the low-Q-value transition to the $9/2^+$ state. The half-life was found to be $(1.97^{+2.24}_{-0.89}) \times 10^7$ years, which makes this candidate feasible for neutrino mass searches.

1. Introduction

The absolute scale of neutrino mass is one of the big open questions in physics. The neutrino-oscillation experiments have demonstrated that at least two of the three flavors of neutrinos have a non-zero mass and for now there are only upper and lower limits on the neutrino mass provided by experiments that in some cases also depend on theoretical models. Stellar observations combined with cosmological models yield an upper limit on the sum of the neutrino masses, which at this point is ~ 0.12 eV/c^2 at 95% confidence level [1]. Several approaches to pinpoint the mass of the neutrino, namely nuclear β and double-β decays [2–4], are based on nuclear decay kinematics.

In all of the kinematical approaches, the neutrino mass is determined via precise measurement of the spectral shape distortion close to the endpoint of the spectrum. Only a very small fraction of the events land near the endpoint and thus it is desirable to study a decay with as small Q value as possible [5]. Smaller the Q value, bigger the fraction of events falling near the endpoint. The KATRIN experiment using tritium (^{3}H) has a ground-state-to-ground-state Q value of 18.6 keV [6] and ^{187}Re has even smaller Q value of about 2.5 keV [7]. ^{163}Ho-nucleus has the lowest known ground-state-to-ground-state electron-capture Q value of about 2.8 keV [8,9]. The rhenium experiment relies on the β transition ^{187}Re$(5/2^+) \rightarrow$ ^{187}Os$(1/2^-)$ which is of the first-forbidden unique type with the lowest known ground-state-to-ground-state β-decay Q value of $2.492(30)_{stat}(15)_{sys}$ keV [7,10]. The Q value of rhenium decay is nearly an order of magnitude smaller than the tritium decay one. Even though all these cases have a very low Q value, they still suffer from the issue that only a very small fraction of decays fall close to the endpoint. In addition, it is necessary to understand the spectrum shape near the endpoint. To detect a

* Corresponding authors.
E-mail addresses: tommi.eronen@jyu.fi (T. Eronen), z.ge@gsi.de (Z. Ge), jouni.t.suhonen@jyu.fi (J. Suhonen).
1 Present address: GANIL, CEA/DSM-CNRS/IN2P3, 14000 Caen, France.

https://doi.org/10.1016/j.physletb.2022.137135

distortion accounting for the mass of a (anti)neutrino, a substantial amount of events are needed with extremely good background suppression and understanding of the detector systematics.

Quite recently, decays that proceed to excited states in the daughter with an ultra-low Q value (considered to be 1 keV or less) have gained interest. These are of interest for future neutrino mass scale determination experiments [11–20]. The existence of a decay with an ultra-low Q value to an excited state in the daughter was first discovered by Cattadori et al. [21] in the β^- decay of ^{115}In. The intriguing decay branch is the β^- decay of the $9/2^+$ ground state of ^{115}In to the $3/2^+$ state in ^{115}In. The Q value of the decay was confirmed to be less than 1 keV by two Penning trap experiments, JYFLTRAP and Florida State University precision Penning-trap mass spectrometer [22,23]. The existence of a decay branch was experimentally confirmed by HADES underground laboratory with the branching ratio of $1.07(17)\times10^{-6}$ [22]. Future experiments to utilize these decays for pinpointing the mass of the neutrino would need to take care of the vast background arising from more dominant (usually ground state) decay branches. One possibility is to use de-exciting gamma rays as a gating transition.

More recently, β^- decay of ^{135}Cs was confirmed to be very similar to ^{115}In by a recent JYFLTRAP Q-value measurement. The Q value to the second excited $11/2^-$ state in ^{135}Ba was measured with JYFLTRAP Penning trap mass spectrometer [24,25] and it is equal to 0.44(31) keV [26]. This confirms that the decay is energetically allowed with an ultra-low Q value. The transition is of first-forbidden unique type with a simple universal spectral shape. The decay has not been experimentally confirmed yet but theoretical partial half-life estimate yields a similar branching ratio ($\sim 10^{-6}$) as for ^{115}In decay. Thus, also ^{135}Cs is a potential candidate for antineutrino-mass measurements.

Here, we report on a new β^- decay Q value of ^{131}I. Prior to our measurement, the ground-state-to-ground-state ($7/2^+ \rightarrow 3/2^+$) Q value is known to be 970.80(60) keV [27,28]. There is a $9/2^+$ state in the ^{131}Xe daughter at 971.22(13) keV, which is potentially fed by the β^- decay of ^{131}I [29,30]. The transition is of allowed type, making it a lucrative candidate since this type of transition is expected to have a reasonable branching ratio and a simple spectral shape. With the available data, a Q value of $-0.42(61)$ keV is deduced. Evidently, it is not possible to conclude whether this transition is energetically possible or not.

The β^- decay Q value of the ground state of ^{131}I to the $9/2^+$ state in ^{131}Xe is simply the ground-state-to-ground-state Q value of ^{131}I minus the energy of the excited state. The excitation energy is already known with 130 eV precision [31] while the Q value is known only to 600 eV precision. The focus of this work was to improve the precision of the ground-state-to-ground-state Q value. This is equivalent to mass difference of ^{131}I and ^{131}Xe, which was measured via direct high-precision cyclotron frequency-ratio determination with the double Penning trap JYFLTRAP.

Based on the new Q value, an estimate of the partial half-life and the branching ratio is derived using wave functions obtained from a nuclear shell-model calculation based on a two-body interaction suitable for the presently discussed mass region. In addition, an analysis of three known allowed β decays was performed in order to compare with the result of the shell-model calculation.

2. Experimental method

The Q value of the ground-state-to-ground-state β^--decay of ^{131}I was measured at the Ion Guide Isotope Separator On-Line facility (IGISOL) with the JYFLTRAP double Penning trap mass spectrometer [25] in the accelerator laboratory of University of Jyväskylä [32,33]. Layout of the facility is shown in Fig. 1. Both the decay parent (^{131}I) and the stable decay daughter (^{131}Xe) ions were simultaneously produced in proton-induced fission reaction.

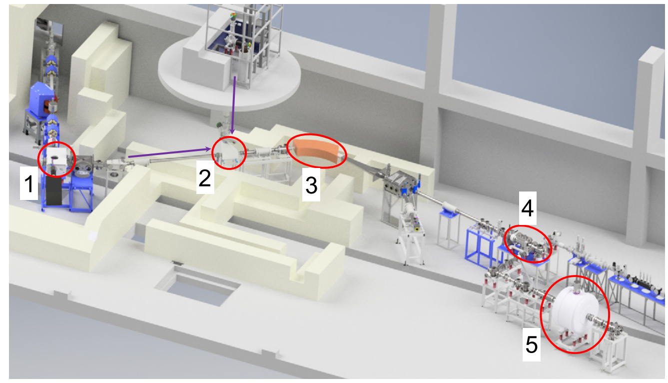

Fig. 1. Layout of the IGISOL facility. The ^{131}I$^+$ and ^{131}Xe$^+$ ions were produced with proton-induced fission reactions at the IGISOL target ion chamber (1). The online beam was selected with an electrostatic kicker (2). The mass number selection was performed with a dipole magnet (3), the ion cooling and bunching in the RFQ cooler-buncher (4) and finally the mass-difference measurement with the JYFLTRAP Penning trap setup (5).

A primary beam of protons with the energy of 30 MeV from the K-130 cyclotron impinged on a uranium target of 15 mg/cm^2 thickness placed inside a gas cell [34]. The secondary products from the fission reactions were stopped in helium gas and extracted with the help of a sextupole radiofrequency ion guide (SPIG) [35]. Through charge-exchange reactions with helium gas and impurities, most of the extracted products were singly charged. After passing the length of the SPIG, the ions are accelerated with 30 kV and guided through a 55° dipole magnet, which has mass resolving power $M/\Delta M \approx 500$. This is sufficient for separation of different isobars in the secondary beam. After the secondary beam has been isobarically separated, the ions of the chosen mass number $A = 131$ containing ^{131}Xe$^+$, ^{131}I$^+$ and other fission fragments having the same mass number are injected into a radiofrequency quadrupole cooler-buncher (RFQ) [36]. The RFQ is used to accumulate, cool and bunch the ions so they can be efficiently injected into JYFLTRAP double Penning trap setup for the actual Q-value measurement.

JYFLTRAP consists of two cylindrical Penning traps which are both situated inside the same 7-T superconducting solenoid. The first trap, performing as the purification and preparation trap, is filled with helium buffer gas and used to remove isobaric contaminants via the sideband buffer gas cooling technique [37]. This technique alone can usually provide sufficient cleaning with a resolving power $M/\Delta M \approx 10^5$ but in this work, an extra cleaning step was required to separate ^{131}I$^+$ and ^{131}Xe$^+$ ions from each other. To prepare a clean sample containing only one isotope, the Ramsey dipolar cleaning technique was utilized [38]. It is imperative for high precision mass measurement that only one ion species is present in the trap when performing the mass measurement to avoid frequency shifts arising, for example, from ion-ion interactions [39]. In the end, the selection of the ion species was a matter of choosing the suitable excitation frequency to either pass the ^{131}I$^+$ or ^{131}Xe$^+$ for the actual mass measurement.

In Penning trap mass spectrometry, the mass m of an ion with charge q is based on the measurement of the cyclotron frequency

$$\nu_c = \frac{1}{2\pi}\frac{q}{m}B, \tag{1}$$

where B is the magnetic field. The best way to deduce the Q value is to measure the cyclotron frequency ratio of the two ions. In this work, singly charged ions were used and the frequency ratio

$$R = \frac{\nu_c(^{131}\mathrm{Xe}^+)}{\nu_c(^{131}\mathrm{I}^+)} = \frac{m(^{131}\mathrm{I}^+)}{m(^{131}\mathrm{Xe}^+)} \tag{2}$$

determined, where $m(^{131}\mathrm{I}^+)$ and $m(^{131}\mathrm{Xe}^+)$ are the masses of the decay daughter ($^{131}\mathrm{I}^+$) and decay parent ($^{131}\mathrm{Xe}^+$) ions, respectively. The ground-state-to-ground-state β^- Q value of $^{131}\mathrm{I}$ is the atomic mass difference of the parent and daughter

$$Q_{\beta^-}(^{131}\mathrm{I}) = \left[M(^{131}\mathrm{I}) - M(^{131}\mathrm{Xe})\right]c^2 \tag{3}$$

and using the frequency ratio from Eq. (2),

$$Q_{\beta^-}(^{131}\mathrm{I}) = (R-1)\left[M(^{131}\mathrm{Xe}) - m_e\right] + \Delta B, \tag{4}$$

where m_e is the mass of an electron and ΔB accounts for the atomic electron binding energy difference (here a few eV).

In this work, the cyclotron frequencies ν_c for the ions were measured using the phase-imaging ion-cyclotron-resonance (PI-ICR) technique [40]. It requires projection of the ion motion in the Penning trap onto a position-sensitive microchannel-plate (MCP) ion detector and provides around 40 times better resolving power than the conventionally used time-of-flight ion-cyclotron-resonance (TOF-ICR) method [40–42]. Measurement scheme 2 described in [41] was applied to directly measure the cyclotron frequency ν_c of the corresponding nuclide.

The cyclotron frequency measurement begins after the ions of interest have been captured into the center of the precision trap. First, coherent components of the magnetron and the axial motions are damped with short RF pulses applied in dipolar configuration. This is followed by the excitation of cyclotron motion using dipolar RF field with the reduced cyclotron frequency (ν_+) to increase the cyclotron radius to about 1 mm. This sets the initial phase of the cyclotron motion.

The next step is the utilization of a quadrupole RF field to convert the cyclotron motion to magnetron motion. For every other measurement cycle the application is done right after the previous step while for every other after a preset longer duration. The cycle with short time interval produces so-called magnetron phase while the longer cycle yields the cyclotron phase. The time difference t of the conversions is called the phase accumulation time. It is known extremely precisely and is the key to high precision frequency determination.

Irrespective of the delay of the conversion excitation, the ions spend same amount of time in the trap before they are extracted towards the MCP detector, which registers the time-of-flight and positions of the ions. The two used time intervals produce two spots of ions on the detector. Combined with a center spot, which is measured without cyclotron and conversion excitations, angles α_- and α_+ for magnetron and cyclotron phases, respectively, are obtained. The time difference between the excitation pulses was chosen to be as close as possible to multiple integer of periods of ion's ν_c frequency (see Eq. (1)) so that the angle difference α_c = α_+ - α_- is as small as possible to minimize systematic shifts to level below 10^{-10} [41]. Finally, the cyclotron frequency is deduced from:

$$\nu_c = \frac{\alpha_c + 2\pi n_c}{2\pi t}, \tag{5}$$

where n_c the number of full revolutions with cyclotron frequency ν_c during the phase accumulation time t.

The cycles with short and long delay before the conversion pulse were alternately applied for a total measurement time of approximately 1 minute with the center spot measured right after. Although the magnetron motion was minimized prior to the measurement and the quadrupole conversion excitation pulse carefully tuned to fully convert the induced cyclotron motion to magnetron, still a tiny fraction of both motions remained. These were taken into account by varying the start of the cyclotron excitation over one magnetron period (≈ 600 μs) and the extraction delay over one cyclotron period (≈ 0.8 μs). Five points in each were chosen and thus one full measurement cycle consisted of 25 points for both the magnetron and cyclotron phases, effectively averaging out any residual motion influence. The collection was repeated for 4 times before switching to the other ion species, for which the cycle was repeated. In total, this was repeated for 3.5 hours for accumulation time t of 399 ms and for 16.5 hours for accumulation time of 500 ms (rounded to the nearest integer of period of ν_c). Fig. 2 shows data with 500 ms accumulation time. The quick changing in timescale of a few minutes, not just between the magnetron and cyclotron spots but also between the two ions, ensured that the magnetic field B is nearly identical for the measurement of both ions, minimizing effect of temporal fluctuation of the field.

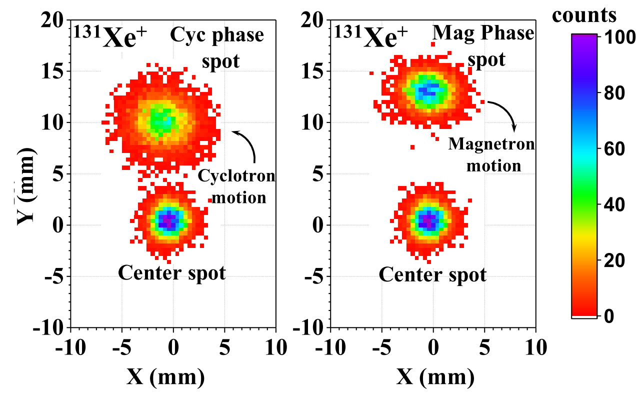

Fig. 2. Ion spots (center, cyclotron phase and magnetron phase) of $^{131}\mathrm{I}^+$ on the 2-dimensional position-sensitive MCP detector after a typical PI-ICR excitation pattern with an accumulation time of 500 ms. The cyclotron phase spot is displayed on the left side and the magnetron phase spot on the right. The angle difference between the two spots relative to the center spot yields α_c of Eq. (5). The color of the pixel represents the number of detected ions.

3. Results and discussion

In total, five sets of data were collected with one using 399 ms of accumulation time and four using 500 ms accumulation time. In each set the measurements of the cyclotron frequencies ν_c of $^{131}\mathrm{Xe}^+$ and $^{131}\mathrm{I}^+$ were interleaved by switching ion species every ≈6 minutes. To obtain their cyclotron frequency ratio R, the values of ν_c of $^{131}\mathrm{Xe}^+$ were linearly interpolated to the time of $^{131}\mathrm{I}^+$ measurement. The frequency ratio for each set was obtained by averaging the individual ratios. Fast switching between the two ion species ensured that the temporal fluctuations of the magnetic field had less than 10^{-10} contribution to the uncertainty [43]. Bunches with up to five detected ions were considered in the data analysis to reduce a possible cyclotron frequency shift due to ion-ion interaction [39,43]. The count-rate related frequency shifts were not observed in the analysis. The frequency shifts in the PI-ICR measurement due to ion image distortions, which were well below the statistical uncertainty, were ignored [41]. Since both ions have the same A/q, the mass-dependent systematic shift, which is due to the imperfections of the electric-quadrupolar field in the Penning trap or a misalignment of the electrostatic trapping field with respect to the magnetic field axis, effectively becomes inferior compared to typical statistical uncertainty achieved in the measurement. The uncertainty of the $M(^{131}\mathrm{Xe})$ is only 8 eV/c^2 and does not contribute to the Q-value uncertainty.

The final frequency ratio was obtained by calculating a weighted mean ratio $\overline{R}$ from the five individual sets. The reduced χ^2 was found to be 1.40, indicating that the statistical uncertainty estimate was too low. To account for this, the uncertainty was expanded by the square root of the reduced chi-squared [44]. The final fre-

Table 1
Potential candidate transitions of ground state of parent nuclei ^{131}I (7/2$^+$) to the excited state of daughter ^{131}Xe with an ultra-low Q value. The first column gives the excited final state of interest for the low Q-value transition. The second column gives decay type. The third column gives the derived experimental decay Q value in units of keV from literature (AME2020) [28] and fourth column lists the Q value from this work. The fifth column gives the experimental excitation energy E* with the experimental error [29]. The sixth column shows the mass excess (ME) in units of keV/c^2 from AME2020 and the last column from this work. Spin-parity of the 971.22(13) keV transition has been confirmed experimentally in [30].

Final state in ^{131}Xe	Decay type	Q value (AME2020)	Q value (This work)	E*	ME (AME2020)	ME (This work)
9/2$^+$	allowed	-0.42(61)	1.03(23)	971.22(13)		
7/2$^+$	allowed	-2.31(62)	-0.86(24)	973.11(14)		
3/2$^+$ (ground state)		970.80(60)	972.25(19)	0	-87442.70(60)	-87441.32(19)

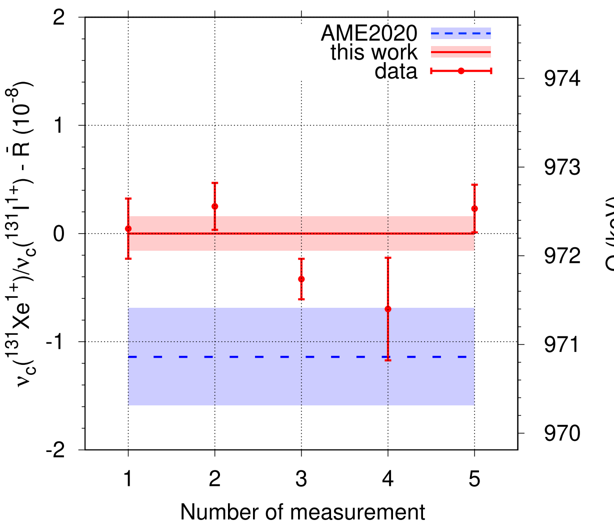

Fig. 3. Cyclotron frequency ratios R of the five sets (points with error bars) and their weighted average compared to the literature value (dashed blue line). The shaded bands show the 1σ uncertainty. The first data point is the set with an accumulation time t = 399 ms while the other four have t = 500 ms. The left axis shows the frequency ratio with zero being the average frequency ratio from this work and the right axis shows the corresponding Q value.

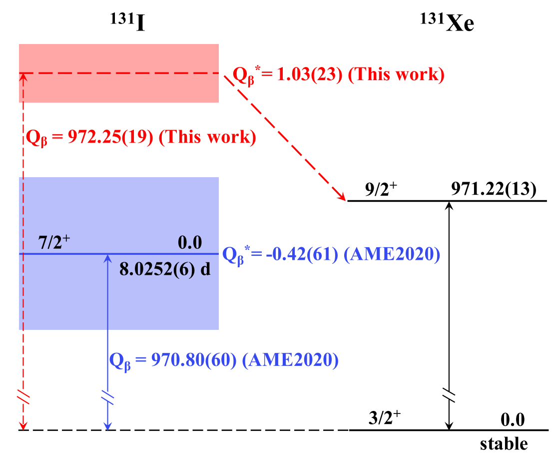

Fig. 4. The ^{131}I ground-state β^- decay to the 971.22(13) keV 9/2$^+$ state in ^{131}Xe. The horizontal blue line depicts the level with the Q_{β^-} taken from AME2020 (shaded area shows the 1σ uncertainty) and the red dashed line the Q_{β^-} from this work. The data for the level scheme are adopted from [27–29].

quency ratio was found to be $\overline{R} = 1.0000079734(16)$. Fig. 3 shows the results of the analysis. Q value for the ground-state-to-ground-state decay and decays to the relevant excited states are tabulated in Table 1 along with the mass excess value of ^{131}I.

The Q value of 972.25(19) keV from this work is more than a factor three more precise than 970.80(60) keV derived from the evaluated masses in AME2020 [27,28]. Also, the Q value is 1.45(63) keV larger. The value in AME2020 originates primarily from the difference between the atomic masses of the parent ^{131}I and that of the daughter ^{131}Xe as listed therein. The ^{131}Xe AME2020 mass value has dominant contribution from a direct Penning trap mass measurement [45], while the adopted AME2020 mass value of ^{131}I was principally derived from a decay measurement of ^{131}I(β^-)^{131}Xe [46,47]. Previous studies have demonstrated that mass values derived in indirect methods, such as decay spectroscopy and nuclear reactions, can suffer from systematic shifts and thus have large discrepancies with values obtained from direct mass measurements [48–50].

The Q values to the excited states near the ground-to-ground-state Q value are obtained by combining the high-precision ground-state-to-ground-state Q value from this work with the excitation energies of the ^{131}Xe states from [29]. The resulting Q values to these low Q value states are given in Table 1 and illustrated in Fig. 4. The decay to the 7/2$^+$ state was found to be energetically forbidden at about 4σ while the decay to the 9/2$^+$ state is energetically possible with more than 3σ confidence, removing the ambiguity of the AME2020-derived Q value whether the decay to the 9/2$^+$ state is energetically allowed or not.

The Q value, 1.03(23) keV, is lower than in presently running or planned direct (anti)neutrino mass experiments (the lowest β^- decay Q value is 2.492(30)$_{\text{stat}}$(15)$_{\text{sys}}$ keV for ^{187}Re and the lowest electron-capture decay Q value is 2.833(30)$_{\text{stat}}$(15)$_{\text{sys}}$ for ^{163}Ho [8]).

To estimate the half-life of this transition, nuclear shell-model (NSM) calculation utilizing the *NuShellX* [51] code with the effective interaction sn100pn used to describe ^{132}Sn [52] with ^{100}Sn as a closed core was used. The single-particle model space 1$g_{7/2}$, 2$d_{5/2}$, 3$s_{1/2}$, 2$d_{3/2}$ and 1$h_{11/2}$ was used for both protons and neutrons. The NSM calculations were able to predict most of the level energies within 100 keV of the corresponding experimental energy below 1 MeV of excitation energy in ^{131}Xe. For the state of interest, 9/2$^+$, the computed excitation energy was 937.0 keV, reasonably close to the experimental energy 971.22(13) keV. The dependence of the Q value to the partial half-life of the 7/2$^+$ $\rightarrow$ 9/2$^+$ transition is illustrated in Fig. 5.

Due to the small Q value of this transition, the corresponding partial half-life is extremely sensitive to the exact value of the decay energy, as evident in Fig. 5 where we depict the computed half-life (dashed line) as a function of the Q value. The colored rectangle represents the NSM-predicted partial half-life (vertical span of the rectangle) for the 9/2$^+$ transition, taking into account the 1σ error in the presently measured Q value (horizontal span of the rectangle). The NSM-predicted half-life reads $(1.97^{+2.24}_{-0.89})$ $\times 10^7$ years.

In order to see how reasonable the half-life prediction of the NSM is, an analysis of the measured log ft values of the well-known allowed transitions to the low-lying 7/2$^+$ and to two 5/2$^+$

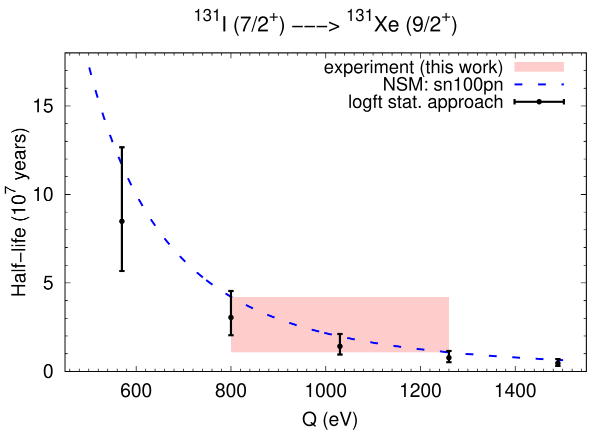

Fig. 5. Shell-model computed half-life as a function of the Q value (dashed line in blue) and the corresponding predicted half-life range for the decay to the $9/2^+$ state (colored rectangle). The points with uncertainties in black are estimates of the half-life assuming the measured Q value 1.03 keV (central point) and its 1σ (points next to the central point) and 2σ errors (points on the extreme left and right), based on a $\log ft$ value deduced using the allowed β transitions to the lower three states in ^{131}Xe (statistical approach, see the text).

states in ^{131}Xe was performed. In this analysis the average of the known $\log ft$ values with their sample standard deviation were used to deduce $\log ft = 6.86(17)$ for the transition to the $9/2^+$ state, in accordance with the NSM calculations. This is called the "statistical approach". The obtained $\log ft$ was then converted to half-life using five values of phase-space factors, calculated for the central value $Q = 1.03$ keV and its 1σ deviations, $Q = 0.80, 1.26$ keV, and 2σ deviations, $Q = 0.57, 1.49$ keV, as shown by the black points in Fig. 5. In the calculation of phase-space factors exact Dirac wave functions with finite nuclear size and electron screening were used in a similar manner previously employed in the case of $\beta^-\beta^-$ decay [53]. The intrinsic uncertainties in the phase-space calculations come from the uncertainty in the nuclear radius and effective charge. However, these uncertainties cause less than 1 percent error in the phase-space factors so that the only non-negligible error comes from the uncertainty in the $\log ft$ value. In Fig. 5, the 1σ error limits of the deduced $\log ft$ are shown as black vertical bars where the error bars are solely from the $\log ft$ standard deviation by the statistical approach. As can be seen, the results agree within error bars with the NSM-computed partial half-life for the $9/2^+$-state transition.

In conclusion, a low Q-value transition was searched for in the β^- decay of ^{131}I to states in ^{131}Xe. Such a low-Q-value transition to the $9/2^+$ state at 971.22(13) keV was now verified by a precise Penning-trap measurement of the mass difference of the two nuclei involved while the transition to the $7/2^+$ state was found to have negative Q value. It should be noted that the energy of the $9/2^+$ state was recently reported to be 972.8(1) keV in [30]. However, this and other energies deviate significantly from the evaluated values [29]. Although we are quite confident in using the evaluated energy of 971.22(13) keV, it is clear that a dedicated, high-precision measurement of the $9/2^+$ state energy is needed to remove any ambiguity.

The decay $7/2^+ \to 9/2^+$ is of allowed type and from the emitted electron spectrum point of view, the transition has a simple universal shape and thus would serve well as a direct electron antineutrino-mass probe. Unfortunately, the estimated partial half-life is so long that the expected decay branch is on the order of 10^{-10}, dominated by β^- decay to $5/2^+$ state at 364.490 keV with $\sim$89% branch. Only time will tell whether future detector technology can overcome the branching problem and lead to a realizable antineutrino-mass experiment on ^{131}I.

Declaration of competing interest

The authors declare that they have no known competing financial interests or personal relationships that could have appeared to influence the work reported in this paper.

Acknowledgements

We acknowledge the support by the Academy of Finland under the Finnish Centre of Excellence Programme 2012-2017 (Nuclear and Accelerator Based Physics Research at JYFL) and projects No. 306980, 312544, 275389, 284516, 295207, 314733, 318043, 327629 and 320062. The support by the EU Horizon 2020 research and innovation program under grant No. 771036 (ERC CoG MAIDEN) is acknowledged.

References

[1] Planck Collaboration, N. Aghanim, Y. Akrami, M. Ashdown, J. Aumont, C. Baccigalupi, M. Ballardini, A.J. Banday, R.B. Barreiro, N. Bartolo, S. Basak, R. Battye, K. Benabed, J.P. Bernard, M. Bersanelli, P. Bielewicz, J.J. Bock, J.R. Bond, J. Borrill, F.R. Bouchet, F. Boulanger, M. Bucher, C. Burigana, R.C. Butler, E. Calabrese, J.F. Cardoso, J. Carron, A. Challinor, H.C. Chiang, J. Chluba, L.P.L. Colombo, C. Combet, D. Contreras, B.P. Crill, F. Cuttaia, P. de Bernardis, G. de Zotti, J. Delabrouille, J.M. Delouis, E.D. Valentino, J.M. Diego, O. Doré, M. Douspis, A. Ducout, X. Dupac, S. Dusini, G. Efstathiou, F. Elsner, T.A. Enßlin, H.K. Eriksen, Y. Fantaye, M. Farhang, J. Fergusson, R. Fernandez-Cobos, F. Finelli, F. Forastieri, M. Frailis, A.A. Fraisse, E. Franceschi, A. Frolov, S. Galeotta, S. Galli, K. Ganga, R.T. Génova-Santos, M. Gerbino, T. Ghosh, J. González-Nuevo, K.M. Górski, S. Gratton, A. Gruppuso, J.E. Gudmundsson, J. Hamann, W. Handley, F.K. Hansen, D. Herranz, S.R. Hildebrandt, E. Hivon, Z. Huang, A.H. Jaffe, W.C. Jones, A. Karakci, E. Keihänen, R. Keskitalo, K. Kiiveri, J. Kim, T.S. Kisner, L. Knox, N. Krachmalnicoff, M. Kunz, H. Kurki-Suonio, G. Lagache, J.M. Lamarre, A. Lasenby, M. Lattanzi, C.R. Lawrence, M.L. Jeune, P. Lemos, J. Lesgourgues, F. Levrier, A. Lewis, M. Liguori, P.B. Lilje, M. Lilley, V. Lindholm, M. López-Caniego, P.M. Lubin, Y.Z. Ma, J.F. Macías-Pérez, G. Maggio, D. Maino, N. Mandolesi, A. Mangilli, A. Marcos-Caballero, M. Maris, P.G. Martin, M. Martinelli, E. Martínez-González, S. Matarrese, N. Mauri, J.D. McEwen, P.R. Meinhold, A. Melchiorri, A. Mennella, M. Migliaccio, M. Millea, S. Mitra, M.A. Miville-Deschênes, D. Molinari, L. Montier, G. Morgante, A. Moss, P. Natoli, H.U. Nørgaard-Nielsen, L. Pagano, D. Paoletti, B. Partridge, G. Patanchon, H.V. Peiris, F. Perrotta, V. Pettorino, F. Piacentini, L. Polastri, G. Polenta, J.L. Puget, J.P. Rachen, M. Reinecke, M. Remazeilles, A. Renzi, G. Rocha, C. Rosset, G. Roudier, J.A. Rubiño-Martín, B. Ruiz-Granados, L. Salvati, M. Sandri, M. Savelainen, D. Scott, E.P.S. Shellard, C. Sirignano, G. Sirri, L.D. Spencer, R. Sunyaev, A.S. Suur-Uski, J.A. Tauber, D. Tavagnacco, M. Tenti, L. Toffolatti, M. Tomasi, T. Trombetti, L. Valenziano, J. Valiviita, B.V. Tent, L. Vibert, P. Vielva, F. Villa, N. Vittorio, B.D. Wandelt, I.K. Wehus, M. White, S.D.M. White, A. Zacchei, A. Zonca, Planck 2018 results, Astron. Astrophys. 641 (2020) A6, https://doi.org/10.1051/0004-6361/201833910.

[2] J. Suhonen, O. Civitarese, Weak-interaction and nuclear-structure aspects of nuclear double beta decay, Phys. Rep. 300 (3–4) (1998) 123–214, https://doi.org/10.1016/S0370-1573(97)00087-2.

[3] F.T. Avignone, S.R. Elliott, J. Engel, Double beta decay, Majorana neutrinos, and neutrino mass, Rev. Mod. Phys. 80 (2) (2008) 481–516, https://doi.org/10.1103/RevModPhys.80.481, arXiv:0708.1033.

[4] H. Ejiri, J. Suhonen, K. Zuber, Neutrino–nuclear responses for astro-neutrinos, single beta decays and double beta decays, Phys. Rep. 797 (2019) 1–102, https://doi.org/10.1016/j.physrep.2018.12.001.

[5] E. Ferri, D. Bagliani, M. Biasotti, G. Ceruti, D. Corsini, M. Faverzani, F. Gatti, A. Giachero, C. Gotti, C. Kilbourne, A. Kling, M. Maino, P. Manfrinetti, A. Nucciotti, G. Pessina, G. Pizzigoni, M. Ribeiro Gomes, M. Sisti, The status of the MARE experiment with 187Re and 163Ho isotopes, Phys. Proc. 61 (August 2015) 227–231, https://doi.org/10.1016/j.phpro.2014.12.037.

[6] E.G. Myers, A. Wagner, H. Kracke, B.A. Wesson, Atomic masses of tritium and helium-3, Phys. Rev. Lett. 114 (1) (2015), https://doi.org/10.1103/PhysRevLett.114.013003.

[7] D.A. Nesterenko, S. Eliseev, K. Blaum, M. Block, S. Chenmarev, A. Dörr, C. Droese, P.E. Filianin, M. Goncharov, E. Minaya Ramirez, Y.N. Novikov, L. Schweikhard, V.V. Simon, Direct determination of the atomic mass difference of Re 187 and Os 187 for neutrino physics and cosmochronology, Phys. Rev. C, Nucl. Phys. 90 (4) (2014) 042501, https://doi.org/10.1103/PhysRevC.90.042501.

[8] S. Eliseev, K. Blaum, M. Block, S. Chenmarev, H. Dorrer, C.E. Düllmann, C. Enss, P.E. Filianin, L. Gastaldo, M. Goncharov, U. Köster, F. Lautenschläger, Y.N. Novikov, A. Rischka, R.X. Schüssler, L. Schweikhard, A. Türler, Direct measurement of the mass difference of ^{163}Ho and ^{163}Dy solves the Q-value puzzle for the neutrino mass determination, Phys. Rev. Lett. 115 (6) (2015) 62501, https://doi.org/10.1103/PhysRevLett.115.062501, arXiv:1604.04210.

[9] P.C. Ranitzsch, C. Hassel, M. Wegner, D. Hengstler, S. Kempf, A. Fleischmann, C. Enss, L. Gastaldo, A. Herlert, K. Johnston, Characterization of the Ho 163 electron capture spectrum: a step towards the electron neutrino mass determination, Phys. Rev. Lett. 119 (12) (2017), https://doi.org/10.1103/PhysRevLett.119.122501.

[10] M. Shamsuzzoha Basunia, Nuclear data sheets for A=193, Nucl. Data Sheets 143 (2017) 1–381, https://doi.org/10.1016/j.nds.2017.08.001.

[11] J. Kopp, A. Merle, Ultralow Q values for neutrino mass measurements, Phys. Rev. C, Nucl. Phys. 81 (4) (2010) 1, https://doi.org/10.1103/PhysRevC.81.045501, arXiv:0911.3329.

[12] S. Eliseev, C. Böhm, D. Beck, K. Blaum, M. Breitenfeldt, V.N. Fedosseev, S. George, F. Herfurth, A. Herlert, H.J. Kluge, M. Kowalska, D. Lunney, S. Naimi, D. Neidherr, Y.N. Novikov, M. Rosenbusch, L. Schweikhard, S. Schwarz, M. Seliverstov, K. Zuber, Direct mass measurements of 194Hg and 194Au: a new route to the neutrino mass determination?, Phys. Lett. B: Nucl. Elem. Part. High-Ener. Phys. 693 (4) (2010) 426–429, https://doi.org/10.1016/j.physletb.2010.08.071, http://www.sciencedirect.com/science/article/B6TVN-50XS6CB-3/2/e50e7350cb45d005a90ae8b4b2c98c1b.

[13] M. Haaranen, J. Suhonen, Beta decay of 115Cd and its possible ultra-low Q-value branch, Eur. Phys. J. A 49 (7) (2013) 1–9, https://doi.org/10.1140/epja/i2013-13093-.

[14] J. Suhonen, Theoretical studies of rare weak processes in nuclei, Phys. Scr. 89 (5) (2014) 54032, https://doi.org/10.1088/0031-8949/89/5/054032.

[15] A. Welker, P. Filianin, N.A. Althubiti, D. Atanasov, K. Blaum, T.E. Cocolios, S. Eliseev, F. Herfurth, S. Kreim, D. Lunney, V. Manea, D. Neidherr, Y. Novikov, M. Rosenbusch, L. Schweikhard, F. Wienholtz, R.N. Wolf, K. Zuber, Precision electron-capture energy in 202Pb and its relevance for neutrino mass determination, Eur. Phys. J. A 53 (7) (2017) 14–17, https://doi.org/10.1140/epja/i2017-12345-y.

[16] J. Karthein, D. Atanasov, K. Blaum, S. Eliseev, P. Filianin, D. Lunney, V. Manea, M. Mougeot, D. Neidherr, Y. Novikov, L. Schweikhard, A. Welker, F. Wienholtz, K. Zuber, Direct decay-energy measurement as a route to the neutrino mass, Hyperfine Interact. 240 (1) (2019) 1–9, https://doi.org/10.1007/s10751-019-1601-z, arXiv:1905.05510.

[17] N.D. Gamage, R. Bhandari, M. Horana Gamage, R. Sandler, M. Redshaw, Identification and investigation of possible ultra-low Q value β decay candidates, Hyperfine Interact. 240 (1) (2019), https://doi.org/10.1007/s10751-019-1588-5.

[18] R. Sandler, G. Bollen, N.D. Gamage, A. Hamaker, C. Izzo, D. Puentes, M. Redshaw, R. Ringle, I. Yandow, Investigation of the potential ultralow Q-value β-decay candidates Sr 89 and Ba 139 using Penning trap mass spectrometry, Phys. Rev. C 100 (2) (2019) 1, https://doi.org/10.1103/PhysRevC.100.024309, arXiv:1906.03335.

[19] Z. Ge, T. Eronen, A. de Roubin, D.A. Nesterenko, M. Hukkanen, O. Beliuskina, R. de Groote, S. Geldhof, W. Gins, A. Kankainen, A. Koszorús, J. Kotila, J. Kostensalo, I.D. Moore, A. Raggio, S. Rinta-Antila, J. Suhonen, V. Virtanen, A.P. Weaver, A. Zadvornaya, A. Jokinen, Direct measurement of the mass difference of ^{72}As-^{72}Ge rules out ^{72}As as a promising β-decay candidate to determine the neutrino mass, Phys. Rev. C 103 (2021) 065502, https://doi.org/10.1103/PhysRevC.103.065502.

[20] Z. Ge, T. Eronen, K.S. Tyrin, J. Kotila, J. Kostensalo, D.A. Nesterenko, O. Beliuskina, R. de Groote, A. de Roubin, S. Geldhof, W. Gins, M. Hukkanen, A. Jokinen, A. Kankainen, A. Koszorús, M.I. Krivoruchenko, S. Kujanpää, I.D. Moore, A. Raggio, S. Rinta-Antila, J. Suhonen, V. Virtanen, A.P. Weaver, A. Zadvornaya, ^{159}Dy electron-capture: a new candidate for neutrino mass determination, Phys. Rev. Lett. 127 (2021) 272301, https://doi.org/10.1103/PhysRevLett.127.272301.

[21] C.M. Cattadori, M. De Deo, M. Laubenstein, L. Pandola, V.I. Tretyak, Observation of β decay of 115In to the first excited level of 115Sn, Nucl. Phys. A 748 (1–2) (2005) 333–347, https://doi.org/10.1016/j.nuclphysa.2004.10.025.

[22] J.S. Wieslander, J. Suhonen, T. Eronen, M. Hult, V.V. Elomaa, A. Jokinen, G. Marissens, M. Misiaszek, M.T. Mustonen, S. Rahaman, C. Weber, J. Äystö, Smallest known Q value of any nuclear decay: the rare β-decay of In115(9/2+)→Sn115(3/2+), Phys. Rev. Lett. 103 (12) (2009) 122501, https://doi.org/10.1103/PhysRevLett.103.122501.

[23] B.J. Mount, M. Redshaw, E.G. Myers, Q value of In115→Sn115(3/2+): the lowest known energy β decay, Phys. Rev. Lett. 103 (12) (2009) 122502, https://doi.org/10.1103/PhysRevLett.103.122502.

[24] A. Kankainen, T. Eronen, D. Nesterenko, A. de Roubin, M. Vilén, Recent experiments at the JYFLTRAP Penning trap, Hyperfine Interact. 241 (1) (2020) 43, https://doi.org/10.1007/s10751-020-01711-5.

[25] T. Eronen, J.C. Hardy, High-precision Q_{EC}-value measurements for superallowed decays, Eur. Phys. J. A 48 (4) (2012) 1–8, https://doi.org/10.1140/epja/i2012-12048-y.

[26] A. De Roubin, J. Kostensalo, T. Eronen, L. Canete, R.P. De Groote, A. Jokinen, A. Kankainen, D.A. Nesterenko, I.D. Moore, S. Rinta-Antila, J. Suhonen, M. Vilén, High-precision Q-value Measurement confirms the potential of Cs 135 for absolute antineutrino mass scale determination, Phys. Rev. Lett. 124 (22) (2020) 1, https://doi.org/10.1103/PhysRevLett.124.222503, arXiv:2002.08282.

[27] W. Huang, M. Wang, F. Kondev, G. Audi, S. Naimi, The AME 2020 atomic mass evaluation (I). Evaluation of input data, and adjustment procedures*, Chin. Phys. C 45 (3) (2021) 030002, https://doi.org/10.1088/1674-1137/abddb0.

[28] M. Wang, W. Huang, F. Kondev, G. Audi, S. Naimi, The AME 2020 atomic mass evaluation (II). Tables, graphs and references*, Chin. Phys. C 45 (3) (2021) 030003, https://doi.org/10.1088/1674-1137/abddaf.

[29] National nuclear data center, Available at https://www.nndc.bnl.gov/, 2021, 2020/4/7.

[30] R. Banik, S. Bhattacharyya, S. Biswas, S. Bhattacharya, G. Mukherjee, S. Rajbanshi, S. Dar, S. Nandi, S. Ali, S. Chatterjee, S. Das, S.D. Gupta, S.S. Ghugre, A. Goswami, A. Lemasson, D. Mondal, S. Mukhopadhyay, H. Pai, S. Pal, D. Pandit, R. Raut, P. Ray, M. Rejmund, S. Samanta, Revealing multiple band structures in ^{131}xe from α-induced reactions, Phys. Rev. C 101 (4) (2020) 044306, https://doi.org/10.1103/physrevc.101.044306.

[31] Y. Khazov, I. Mitropolsky, A. Rodionov, Nuclear data sheets for A = 131, Nucl. Data Sheets 107 (11) (2006) 2715–2930, https://doi.org/10.1016/j.nds.2006.10.001.

[32] I.D. Moore, T. Eronen, D. Gorelov, J. Hakala, A. Jokinen, A. Kankainen, V.S. Kolhinen, J. Koponen, H. Penttilä, I. Pohjalainen, M. Reponen, J. Rissanen, A. Saastamoinen, S. Rinta-Antila, V. Sonnenschein, J. Äystö, Towards commissioning the new IGISOL-4 facility, Nucl. Instrum. Methods Phys. Res., Sect. B, Beam Interact. Mater. Atoms 317 (PART B) (2013) 208–213, https://doi.org/10.1016/j.nimb.2013.06.036, http://www.sciencedirect.com/science/article/pii/S0168583X13007143.

[33] V.S. Kolhinen, T. Eronen, D. Gorelov, J. Hakala, A. Jokinen, K. Jokiranta, A. Kankainen, M. Koikkalainen, J. Koponen, H. Kulmala, M. Lantz, A. Mattera, I.D. Moore, H. Penttilä, T. Pikkarainen, I. Pohjlainen, M. Reponen, S. Rinta-Antila, J. Rissanen, C. Rodríguez Triguero, K. Rytkönen, A. Saastamoinen, A. Solders, V. Sonnenschein, J. Äystö, Recommissioning of JYFLTRAP at the new IGISOL-4 facility, Nucl. Instrum. Methods Phys. Res., Sect. B, Beam Interact. Mater. Atoms 317 (PART B) (2013) 506–509, https://doi.org/10.1016/j.nimb.2013.07.050.

[34] H. Penttilä, D. Gorelov, V.V. Elomaa, T. Eronen, U. Hager, J. Hakala, A. Jokinen, A. Kankainen, P. Karvonen, I.D. Moore, J. Parkkonen, K. Peräjärvi, I. Pohjalainen, S. Rahaman, S. Rinta-Antila, J. Rissanen, V.A. Rubchenya, A. Saastamoinen, V. Simutkin, T. Sonoda, C. Weber, A. Voss, J. Äystö, Independent isotopic yields in 25 MeV and 50 MeV proton-induced fission of natU, Eur. Phys. J. A 52 (4) (2016) 104, https://doi.org/10.1140/epja/i2016-16104-4.

[35] P. Karvonen, I.D. Moore, T. Sonoda, T. Kessler, H. Penttilä, K. Peräjärvi, P. Ronkanen, J. Äystö, A sextupole ion beam guide to improve the efficiency and beam quality at IGISOL, Nucl. Instrum. Methods Phys. Res., Sect. B, Beam Interact. Mater. Atoms 266 (21) (2008) 4794–4807, https://doi.org/10.1016/j.nimb.2008.07.022, http://www.sciencedirect.com/science/article/B6TJN-4T2S8KR-1/2/1d7624cd369335096dcb1fd81a410fea.

[36] A. Nieminen, J. Huikari, A. Jokinen, J. Äystö, P. Campbell, E.C. Cochrane, Beam cooler for low-energy radioactive ions, Nucl. Instrum. Methods Phys. Res., Sect. A, Accel. Spectrom. Detect. Assoc. Equip. 469 (2) (2001) 244–253, https://doi.org/10.1016/S0168-9002(00)00750-6, http://www.sciencedirect.com/science/article/B6TJM-43PGJKX-C/1/93d5587efba5cfe8571b63228952dab8.

[37] G. Savard, S. Becker, G. Bollen, H.J. Kluge, R.B. Moore, T. Otto, L. Schweikhard, H. Stolzenberg, U. Wiess, A new cooling technique for heavy ions in a Penning trap, Phys. Lett. A 158 (5) (1991) 247–252, https://doi.org/10.1016/0375-9601(91)91008-2.

[38] T. Eronen, V.V. Elomaa, U. Hager, J. Hakala, A. Jokinen, A. Kankainen, S. Rahaman, J. Rissanen, C. Weber, J. Äystö, JYFLTRAP: mass spectrometry and isomerically clean beams, Acta Phys. Pol. B 39 (2) (2008) 445–455, https://www.actaphys.uj.edu.pl/R/39/2/445/pdf.

[39] A. Kellerbauer, K. Blaum, G. Bollen, F. Herfurth, H.J. Kluge, M. Kuckein, E. Sauvan, C. Scheidenberger, L. Schweikhard, From direct to absolute mass measurements: a study of the accuracy of ISOLTRAP, Eur. Phys. J. D 22 (1) (2003) 53–64, https://doi.org/10.1140/epjd/e2002-00222-0.

[40] D.A. Nesterenko, T. Eronen, A. Kankainen, L. Canete, A. Jokinen, I.D. Moore, H. Penttilä, S. Rinta-Antila, A. de Roubin, M. Vilen, Phase-imaging ion-cyclotron-resonance technique at the JYFLTRAP double Penning trap mass spectrometer., Eur. Phys. J. A 54 (9) (2018) 0, https://doi.org/10.1140/epja/i2018-12589-y.

[41] S. Eliseev, K. Blaum, M. Block, A. Dörr, C. Droese, T. Eronen, M. Goncharov, M. Höcker, J. Ketter, E.M. Ramirez, D.A. Nesterenko, Y.N. Novikov, L. Schweikhard, A phase-imaging technique for cyclotron-frequency measurements, Appl. Phys. B, Lasers Opt. 114 (1–2) (2014) 107–128, https://doi.org/10.1007/s00340-013-5621-0.

[42] S. Eliseev, K. Blaum, M. Block, C. Droese, M. Goncharov, E. Minaya Ramirez, D.A. Nesterenko, Y.N. Novikov, L. Schweikhard, Phase-imaging ion-cyclotron-resonance measurements for short-lived nuclides, Phys. Rev. Lett. 110 (8) (2013) 82501, https://doi.org/10.1103/PhysRevLett.110.082501.

[43] C. Roux, K. Blaum, M. Block, C. Droese, S. Eliseev, M. Goncharov, F. Herfurth, E.M. Ramirez, D.A. Nesterenko, Y.N. Novikov, L. Schweikhard, Data analysis of Q-value measurements for double-electron capture with SHIPTRAP, Eur. Phys. J. D 67 (7) (2013) 1–9, https://doi.org/10.1140/epjd/e2013-40110-x.

[44] R.T. Birge, The calculation of errors by the method of least squares, Phys. Rev. 40 (2) (1932) 207–227, https://doi.org/10.1103/PhysRev.40.207.

[45] M. Höcker, R. Rana, E.G. Myers, Atomic masses of 82, 83Kr and 131,134Xe, Phys. Rev. A 88 (5) (2013) 52502, https://doi.org/10.1103/PhysRevA.88.052502.

[46] N. Verster, G. Nijgh, R. van Lieshout, C. Bakker, Measurement of the radiations from 131i and 131xe with a lens type beta-ray spectrometer, Physica 17 (7) (1951) 637–657, https://doi.org/10.1016/0031-8914(51)90048-1.

[47] D. Rose, G. Hinman, L.G. Lang, Internal conversion in i^{131}, Phys. Rev. 86 (1952) 863–865, https://doi.org/10.1103/PhysRev.86.863.

[48] J.C. Hardy, L.C. Carraz, B. Jonson, P.G. Hansen, The essential decay of pandemonium: a demonstration of errors in complex beta-decay schemes, Phys. Lett. B 71 (2) (1977) 307–310, https://doi.org/10.1016/0370-2693(77)90223-4.

[49] S. Eliseev, D. Nesterenko, K. Blaum, M. Block, C. Droese, F. Herfurth, E. Minaya Ramirez, Y.N. Novikov, L. Schweikhard, K. Zuber, Q values for neutrinoless double-electron capture in 96Ru, 162Er, and 168Yb, Phys. Rev. C, Nucl. Phys. 83 (3) (2011) 38501, https://doi.org/10.1103/PhysRevC.83.038501.

[50] D.A. Nesterenko, L. Canete, T. Eronen, A. Jokinen, A. Kankainen, Y.N. Novikov, S. Rinta-Antila, A. de Roubin, M. Vilen, High-precision measurement of the mass difference between ^{102}Pd and ^{102}Ru, Int. J. Mass Spectrom. 435 (2019) 204–208, https://doi.org/10.1016/j.ijms.2018.10.038.

[51] B. Brown, W. Rae, The shell-model code NuShellX@MSU, Nucl. Data Sheets 120 (2014) 115–118, https://doi.org/10.1016/j.nds.2014.07.022.

[52] B.A. Brown, N.J. Stone, J.R. Stone, I.S. Towner, M. Hjorth-Jensen, Magnetic moments of the 2 states around 132sn, Phys. Rev. C 71 (4) (2005), https://doi.org/10.1103/physrevc.71.044317.

[53] J. Kotila, F. Iachello, Phase-space factors for double-β decay, Phys. Rev. C 85 (2012) 034316, https://doi.org/10.1103/PhysRevC.85.034316.